Research Papers
Issue RP0179
September 2013

ISC - Impacts on Soil and Coasts Division

GCM driven COSMO-CLM post-processed precipitation over Italy: control and future scenarios

By **Marco Turco**
Impacts on Soil and Coasts Division, CMCC
marco.turco@cmcc.it

Alessandra Lucia Zollo
Impacts on Soil and Coasts Division, CMCC
alessandra.zollo@cmcc.it

Valeria Rillo
Impacts on Soil and Coasts Division, CMCC
valeria.rillo@cmcc.it

and **Paola Mercogliano**
Impacts on Soil and Coasts Division, CMCC;
Italian Aerospace Research Center, CIRA
paola.mercogliano@cmcc.it

SUMMARY In Turco et al. (2013a, [19]), three MOS methods (Linear-Scaling, Quantile-Mapping and MOS Analog) have been proposed and they have shown skill to downscale daily precipitation outputs of the ERA40-driven COSMO-CLM model over three Italian domain (Orvieto, Po river basin, Sardinia). This study extend this previous analysis [19] applying these MOS techniques to the entire model chain (CMCC-CM driven COSMO-CLM model) in control and future periods. These methods clearly outperform the uncalibrated RCM outputs, regardless of the region, the season and precipitation index. Generally, better results have been obtained with the quantile mapping method. Finally, the application of these MOS techniques to future RCM scenarios is also discussed. Generally the projected scenarios are quite consistent among the dynamical model and the MOS methods, giving some confidence in the robustness of the MOS in changing climate conditions. The stronger climate change signal that appears, regardless of the scenario (RCP4.5 or RCP8.5), domain, downscaling method or precipitation indices, is the decreasing trend in summer. This report presents the preliminary results of combined downscaling methods for precipitation, adopted by CMCC within the framework of the GEMINA project (product P93b).

This report represents the Deliverable P93b developed within the framework of Work Package 6.2.17 of the GEMINA project, funded by the Italian Ministry of Education, University and Research and the Italian Ministry of Environment, Land and Sea. The authors would also like to thank NEXTDATA project for supporting this research.

INTRODUCTION

Regional quantitative scenarios of possible precipitation changes are necessary to assess their potential impacts in the future and their development is a strategic topic in several international and national climate programs. Precipitation is a major factor in crucial sectors such as agriculture and hydrology, but at the same time, it is one of the variables with the greatest uncertainty in numerical models. These considerations are exacerbated when the extremes are considered. At global scale, although there are still significant uncertainties and despite the complexity of the task, the Global Circulation Models (GCMs) generally project an increase in precipitation extreme under different anthropogenic forcing scenarios [9, 13], that are consistent with theoretical basis [2]. However, the GCM coarse resolution (generally few hundred kilometers) it is not suitable to analyse the scenario at regional scale (generally few tens kilometers). Usually the gap between the coarse resolution GCMs and the appropriate scale for regional climate studies is bridged by means of dynamical and/or statistical downscaling techniques [4, 21, 1, 8].

In a previous study, Turco et al. (2013a, [19]) evaluated three different MOS (Model Output Statistics) methods to refine the precipitation output of the ERA40-driven COSMO-CLM model. They focus on the mean and extreme precipitation regimes over three Italian areas (Fig. 1): Orvieto, Sardenia and Po river basin. The three methods tested are of increasing complexity: (i) the simple linear-scaling (LS), (ii) the quantile mapping (QM), and (iii) the MOS Analog method (MA, [18]). This comparison was performed under "perfect boundary condition", that is, the lateral boundary conditions are provided by ERA40 reanalysis data, in order to reduce the influence of the errors related to the GCM. Their analysis indicates that the application of MOS techniques generally improves the outputs of the COSMO-CLM model, and, among the MOS methods, better results have been generally obtained with the quantile mapping method.

The application of these MOS method to downscale future RCM scenarios (driven by GCMs simulations) is technically straightforward. However, before to develop the future scenarios, since RCMs are also limited to the quality of the GCM boundary condition, it is important to analyze these methods applied to the entire GCM-RCM model chain in a control period. Besides, it is also important test the robustness of the downscaling methods in climate change conditions.

Taking these considerations into account, the objectives of the present study are, first, to evaluate if the GCM-RCM-MOS chain is able to reproduce the observed climate patterns of mean and extreme precipitation, and, second, to analyse the consistency of the climate change signals of the RCM and the MOS as a first test of the stationarity of the MOS methods. Indeed the climate change signals of the GCM-RCM and of the GCM-RCM-MOS should be similar since the statistical scenarios are driven by the dynamical model ones.

The study is organized as follows. After this Introduction, Section "Data and Methods" describes the observed and simulated data and the three MOS methods are presented. Then, the Sections "Control period results" analyses the validation results in a control period. Finally, Section "Future scenarios" presents the scenarios results and Section "Conclusion" resumes the main findings of this report.

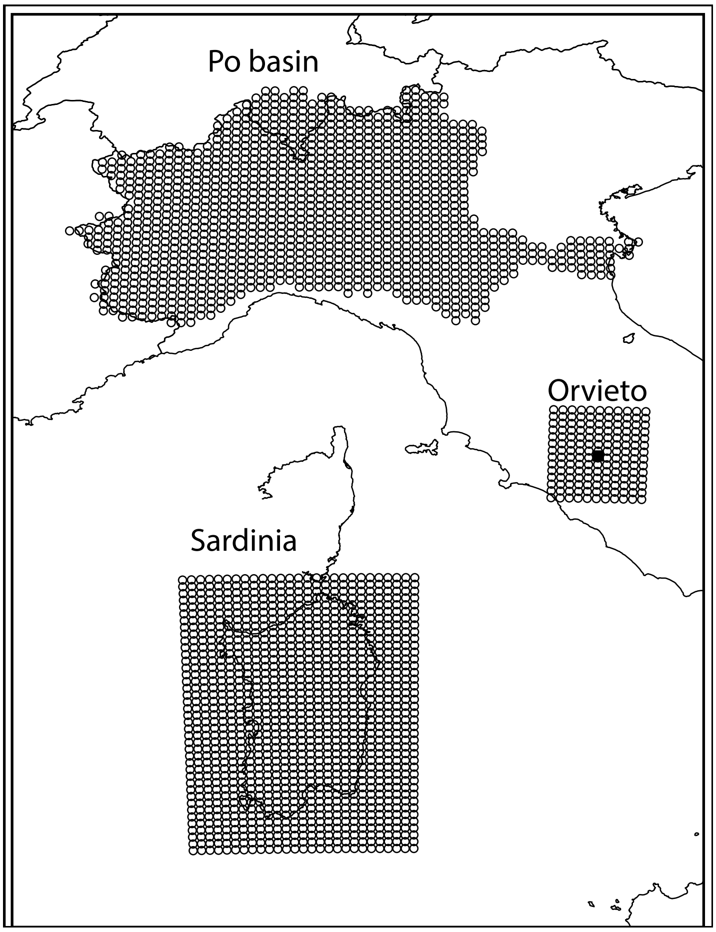

Figure 1:
The three domains of the study: (i) Orvieto, (ii) Po river basin, (iii) Sardinia. The black circles indicate the gridpoints of the COSMO-CLM model over these areas used in the MOS approaches. The black filled square indicates the position of the Orvieto station.

DATA AND METHODS

COSMO-CLM REGIONAL CLIMATE MODEL

In this study, we consider the CMCC-CM driven COSMO-CLM model [12] both for the control period (1971-2000) and for a future period up to 2100. The CMCC-CM global model [14] is the coupled atmosphere-ocean general circulation model adopted by CMCC; its atmospherical component is ECHAM5, that has a horizontal resolution of $0.75°$ (about 85 km), 31 vertical levels and 4 soil levels. The COSMO-CLM regional climate model is the climate version of the COSMO-LM non-hydrostatic limited area model [15]. A detailed description of this RCM and its evaluation is given in Zollo et al. (2012, [22]). The horizontal resolution of the performed simulations is $0.0715°$ (about 8 km). The model domain is $3°$-$20°$E / $36°$-$50°$N. Table 1 summarizes the main features of the COSMO-CLM set-up. Two different IPCC scenarios have been considered for the future period: RCP4.5 and RCP8.5. RCP stands for Representative Concentration Pathways; the RCP4.5 is characterized by a radiative forcing of about 4.5 W/m^2 at stabilization after 2100, while the RCP8.5 has a radiative forcing higher than 8.5 W/m^2 in 2100.

Driving data	CMCC-CM
Horizontal resolution	$0.0715°$ (about 8km)
Num. of grid points	224 x 230
Num. of vertical levels in the atm.	40
Num. of soil levels	7
Soil scheme	TERRA_ML
Time step	40 s
Melting processes	yes
Convection scheme	TIEDTKE
Frequency of radiation computation	1 hour
Time integration	Runge-Kutta (3rd ord.)
Frequency update boundary cond.	6 hours

Table 1
Main features of the COSMO-CLM set-up.

OBSERVED DATA

As mentioned in the Introduction, the three domains of this study are: (i) Orvieto, (ii) Po river basin, (iii) Sardinia (Fig. 1). These are interesting domains to study the impact of climate change on the hydro-geological risk, and, besides, they are also covered by high-resolution data over the baseline period 1971-2000. In the following these data are briefly described. The readers are referred to Turco et al. (2013a,[19]) for more details on these data.

Orvieto. Orvieto is an historical town located at about 100 km north of Rome. Orvieto represents an excellent case study to estimate the impact of climate change on landslide risk. The observed data of daily precipitation from the Orvieto station are used. The rainfall values time series result quite complete; major gaps concern parts of the years 1966,1979 and 1980; for these ones, the data are replaced by measurements supplied by Acquapendente station (about 20 km away from the Orvieto station).

Po river basin. The Po river basin is characterized by a great variability of precipitation regimes due to the influences of different climatological regimes, such as the Mediterranean, Continental, Atlantic, and Polar. In addition, precipitation plays a major role in water resources and natural hazards in this area, with high hydro-geological risk and strong human pressure. The observed data of daily precipitation are provided by ARPA Emilia Romagna over a gridded dataset, called EMR. This recently developed gridded dataset that covers the Po basin, is based on 1128 quality controlled precipitation stations. The rain gauges network is sufficiently dense (on average around one station per 60 km2) to produce a grid at $0.0715°$ (about 8 km), that is, the same of the nominal horizontal resolution of the COSMO-CLM model. This observed dataset was positively evaluated by Turco et al. (2013b, [20]) by comparing it to other two high-resolution datasets of interpolated precipitation (EOBS [6], MAP [3]).

Sardinia. The Sardinia island is highly vulnerable to flash flooding and landslides and it is challenging domain to perform precipitation downscaling also because this field is highly variable in this relatively small area. The observed data used for this domain are 39 time series of daily cumulated precipitation managed by *Ente Idrografico della Sardegna*. This dataset has been kindly provided by the CMCC IAFENT division (Sassari).

MOS METHODS

Here we briefly describe the three MOS methods that we compare: (i) the linear-scaling, (ii) the quantile mapping, and (iii) the MOS Analog method (see Turco et al., 2013a,[19] for more details).

First, the linear-scaling approach consists in correcting the monthly differences between observed and simulated values. The quantile mapping correction, instead, tries to adjust all the moments of the probability distribution function (PDF) of the precipitation field. The idea is to calculate the correct variable as a function of the original simulated variable using a transfer function calculated forcing the equality between the CDF (cumulative distribution function) of the observed and simulated variables [11]. We applied the quantile mapping assuming that both observed and simulated distributions are well approximated by a Gamma distribution. This distribution is commonly used for representing the PDF of precipitation [10] and several studies have proved that it is effective for modeling rainfall data ([17], [7], [5]). Finally, the MOS analog method (MA, [18])), is based on the hypothesis that "analogue" weather patterns should cause "analogue" local effects. It consists in a two steps procedure: for each day to be downscaled in a test period, first the closest historical predictor (the RCM precipitation, i.e. the analog) is found and then the observed local precipitation, correspondent to the analog day, is used as downscaled precipitation.

CONTROL PERIOD RESULTS

We evaluate the ability of the CMCC-CM-driven COSMO-CLM model and of the post-processing methods to reproduce the seasonal climatology (spatial pattern) for three precipitation indices proposed by ETC-CDI (http://cccma.seos.uvic.ca/ETCCDI) and shown in Table 2.

Label	Description	Units
PRCPTOT	total precipitation	mm
R1	number of days with precipitation over 1 mm/day	days
RX1DAY	maximum precipitation in 1 day	mm

Table 2
Climatic mean and extreme ETCCDI indices for precipitation used in this work (see also http://cccma.seos.uvic.ca/ETCCDI).

The comparisons between the simulated and observed climatologies are resumed by the Taylor diagram [16]. This diagram consents to synthesize three metrics of spatial similarity, i.e. standard deviation (S), centered root-mean-square difference (R) and correlation (C), in a single bidimensional plot. Two variations from the standard Taylor diagram have been applied in this study:

- The statistics were normalized dividing, both the centered root mean square error and the standard deviations of the simulated fields, by the standard deviation of the observations. In this way it is possible to compare the different indices.

- To include information about overall biases (M), the colour of each point indicates the difference between the simulated and observed mean, normalized by the observed mean.

ORVIETO

As in Turco et al. (2013a,[19]) the linear-scaling and the quantile mapping methods are here applied to the ensembles of grid-points that surround the station in a square of 1° (see Fig. 1), in order to take into account the reliable scale of the model. Indeed it should be noted that the direct model output is not a point value but an average (over a grid) value, reliable considering only from 4 to 10 times the nominal resolution of the model.

Figure 2 shows the comparison in terms of probability distribution, CDF (top) and PDF (bottom) of the three proposed methods. The QM method has a better agreement with the observation than the LS and MA methods, whose performance are not satisfactory. A closer look at the performances of the RCM and the three methods in reproducing the climatological values of the three indices considered (described in Table 2), is given in Table 3. These results show that the COSMO-CLM model underestimate the $PRCPTOT$ index in summer and autumn, and overestimate the number of rainy days in winter and spring. The results are surprisingly good for LS and QM, in particular for QM the observed value is always within the range (5° and 90° percentile of the ensembles of grid-points that surround the station in a square of 1°) of the QM simulated values, regardless the season or the index. Finally, the MA method has quite good performances in terms of $R1$ and $RX1DAY$, but has worst performances in terms of total precipitation, indeed it shows an overestimation in winter and spring and a strong underestimation in autumn.

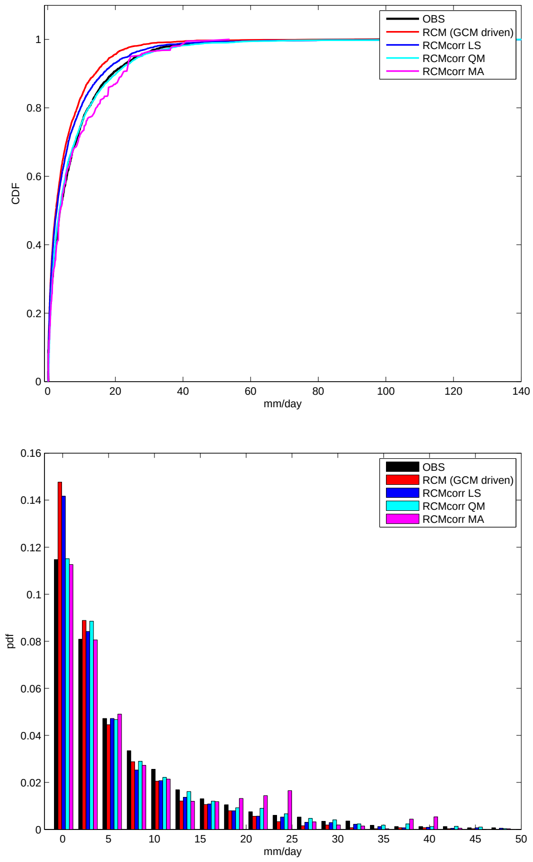

Figure 2:
Probability distributions of precipitation values for observations (OBS), original RCM, and corrected RCM with the three proposed methods: Linear-Scaling (LS), Quantile mapping (QM) and MOS analogs (MA). The first figure is relative to the CDF and the second one to the PDF. For both original and corrected simulations the nearest grid point to Orvieto station has been considered.

		DJF	MAM	JJA	SON
PRCPTOT (mm)	**OBS**	184	190	114	268
	RCM	202 (145,255)	181 (142,239)	61 (36 ,88)	188 (131,245)
	LS	187 (155,213)	193 (157,225)	121 (71,165)	272 (209,327)
	QM	190 (149,225)	196 (151,238)	117 (79,154)	273 (208,330)
	MA	204	250	105	187
R1 (days)	**OBS**	21	22	12	21
	RCM	27 (23,30)	28 (23,32)	8 (6,11)	20 (17,23)
	LS	26 (23,29)	28 (23,31)	10 (8,13)	21 (18,24)
	QM	21 (18,24)	23 (19,26)	13 (10,15)	21 (18,24)
	MA	22	24	10	17
RX1DAY (mm/day)	**OBS**	32	29	29	50
	RCM	28 (18,39)	24 (16,37)	23 (9,33)	38 (21,57)
	LS	27 (18,36)	26 (17,37)	47 (18 ,69)	55 (31,79)
	QM	36 (23,50)	34 (21,51)	37 (16,52)	56 (32,81)
	MA	32	35	29	38

Table 3

Seasonal means for the three indices $PRCPTOT$, $R1$ and $RX1DAY$, for the Orvieto domain. The mean value for each index and for each season, averaged over the period 1971-2000, is shown. The values are relative to observations (OBS), original simulation (RCM) and corrected simulations using linear scaling (LS), quantile mapping (QM) and MOS analog (MA) methods. For RCM, LS and QM the nearest grid point to Orvieto station has been considered together with 5° and 90° percentile (in brackets) of the ensembles of grid-points that surround the station in a square of 1°; for OBS and MA, instead, only one value is available.

PO RIVER BASIN

For illustrative purpose, the results for the winter season (DJF) are summarised in Figure 3 through comparison maps for the observed dataset (left column), the COSMO-CLM model (center) and the corresponding correction using the quantile mapping method (right column). Each row is representative of one index, $PRCPTOT$ (top), $R1$ (middle), and $RX1DAY$ (bottom). The seasonal values of the indices are averaged over the common period 1971-2000. Below each subplot is indicated the bias (or mean error M), relative standard deviations (S), the centered root-mean-square (R) and the correlation (C), for the QM method and for the COSMO-CLM model. Please notice that these numbers indicate the similarity scores used in the following Taylor diagrams. Figure 3 shows an overestimation of the COSMO-CLM model in terms of total precipitation (62 %), number of rainy days (44 %) and maximum precipitation in one day (11 %). The overestimation is larger over the mountains areas (Alps and Apennines). In addition to the model chain limitations, this overestimation could also be related to the well-known problem in measuring the winter precipitation at high altitudes. The QM values show a higher agreement with the observations and clearly outperform the uncalibrated RCM outputs for all the indices (Fig. 3).

To summarize the results for all the methods, seasons and indices, the spatial similarity of the simulated values in reproducing the observed climatologies of the ETCCDI indices is shown in the Taylor diagrams displayed in Fig. 4. The quantile mapping method have the best scores for most indices and seasons, while the direct model output shows the worst results in most cases. As for the ERA40-driven run ([19]) the MA method also reduced the bias of the RCM, except for the autumn season, when the MOS analog shows an underestimation (ranging from 10 to 20%) of the observed values. The LS method generally shows the worst results among the three MOS method, although it improves the representation of the $PRCPTOT$ index, as expected, and also the other two indices, to a lesser extent.

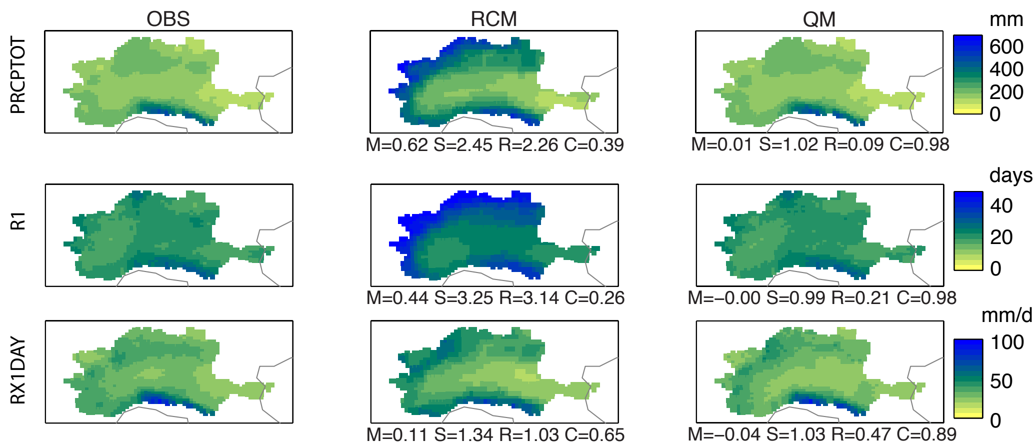

Figure 3:
Spatial distribution of the observed (left), COSMO-CLM (central) and downscaled (right) mean values (averaged over the control period 1971-2000) for the winter precipitation indices shown in Table 2. The spatial validation scores for the RCM and QM simulated values are given below the corresponding panels: bias (or mean error M), relative standard deviations (S), correlation (C) and centred root-mean-square (R).

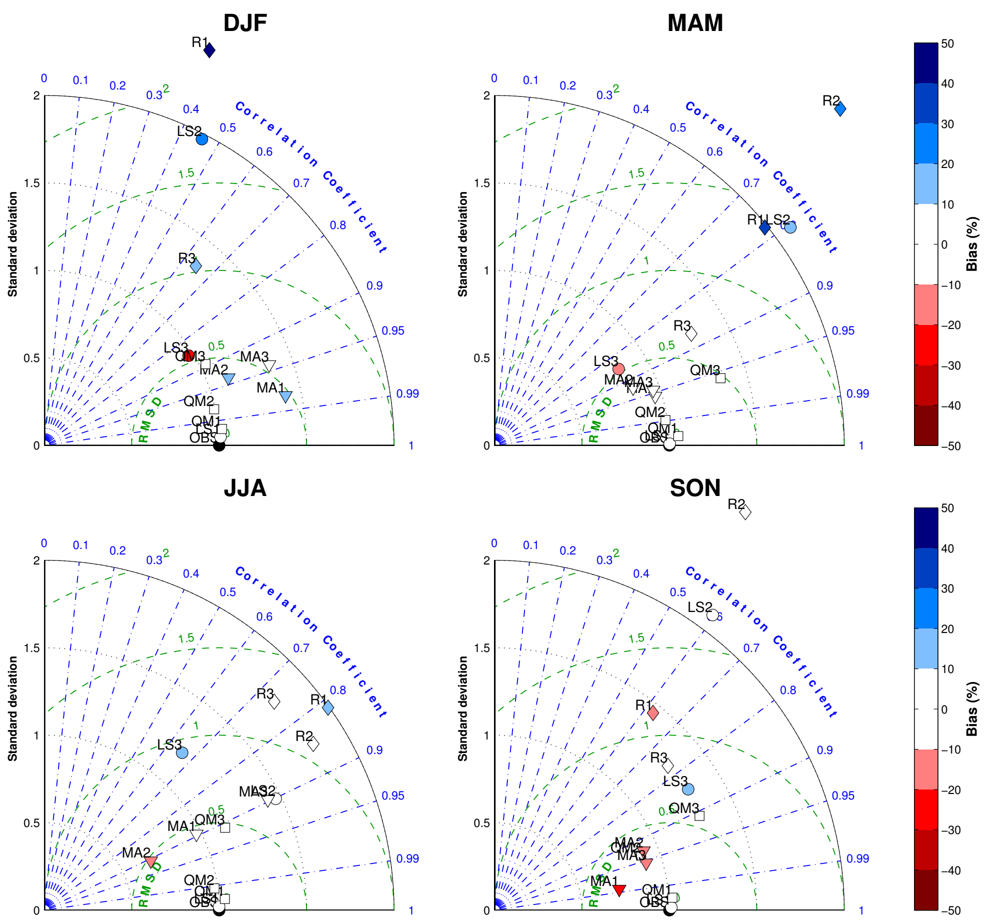

Figure 4:
Taylor diagrams for the seasonal precipitation climatology over the Po river basin. Better results are closer to observation (OBS). The circles with LS are used for the linear-scaling method, the squares with QM for the quantile mapping, the triangles with MA for the MOS analogs method, while the diamonds with R for the RCM. The colours indicate the bias (in percentage respect to the Observed mean). The numbers correspond to the different indices: 1=PRCPTOT; 2=R1; 3=RX1DAY.

SARDINIA

Figure 5 shows an illustrative example of the comparison maps for the COSMO-CLM model and the corresponding MOS analog values for the three indices considered for the autumn season. The panels in this figure show the seasonal values of the three indices (averaged in the control period 1971-2000) for the observed data (first column), the RCM (second column) and the MOS analog downscaled values (third column); the numbers below the figures indicate the spatial metrics used also in the Taylor diagram. This figure shows that the MOS analog downscaled values clearly outperform the uncalibrated RCM outputs.

Figure 6 summarizes the verification results for all the MOS methods, seasons and indices. This figure shows that, overall, the three MOS methods dramatically improve the RCM results, especially for the MA and QM method. For the LS the improvement is smaller than for the previous methods.

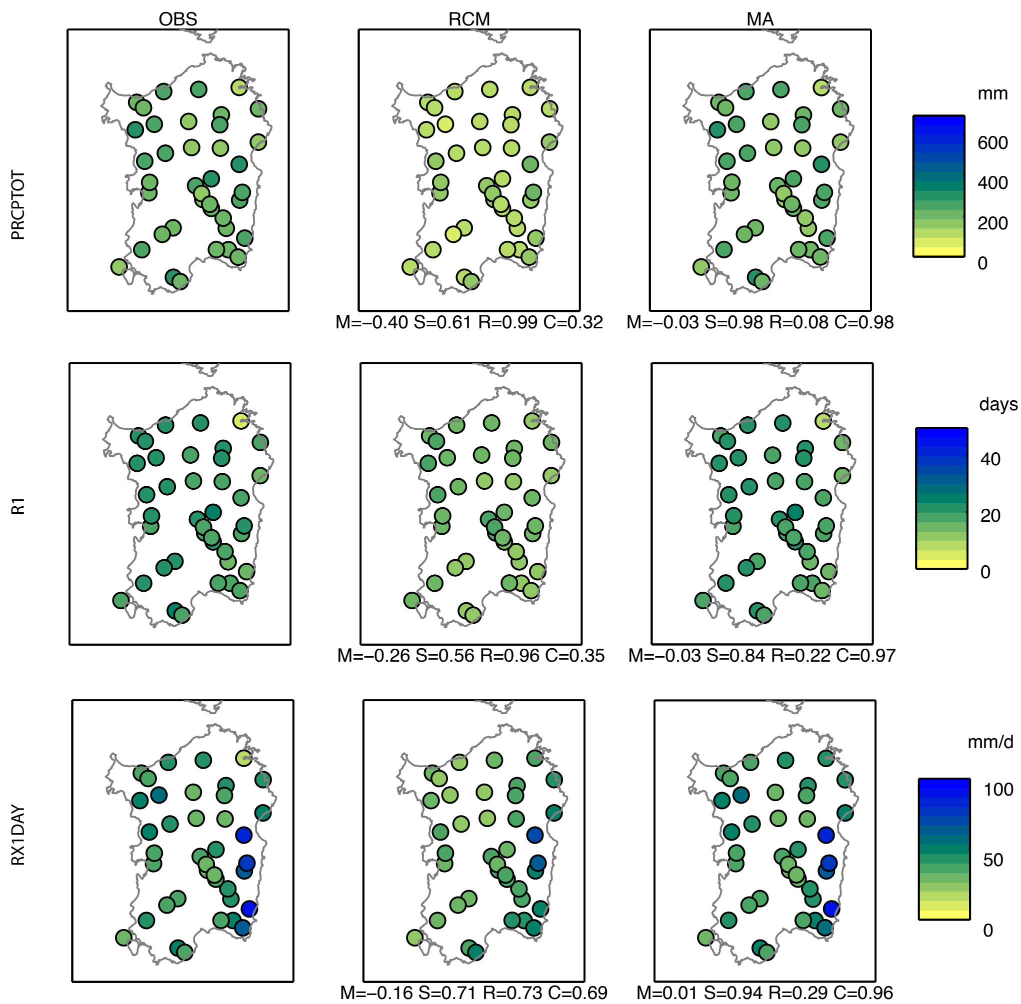

Figure 5:
Spatial distribution of the observed (left), COSMO-CLM (central) and downscaled (right) mean values (averaged over the control period 1971-2000) for the autumn precipitation indices shown in Table 2. The spatial validation scores for the RCM and MOS $analog$ simulated values are given below the corresponding panels: bias (or mean error M), relative standard deviations (S), correlation (C) and centred root-mean-square (R).

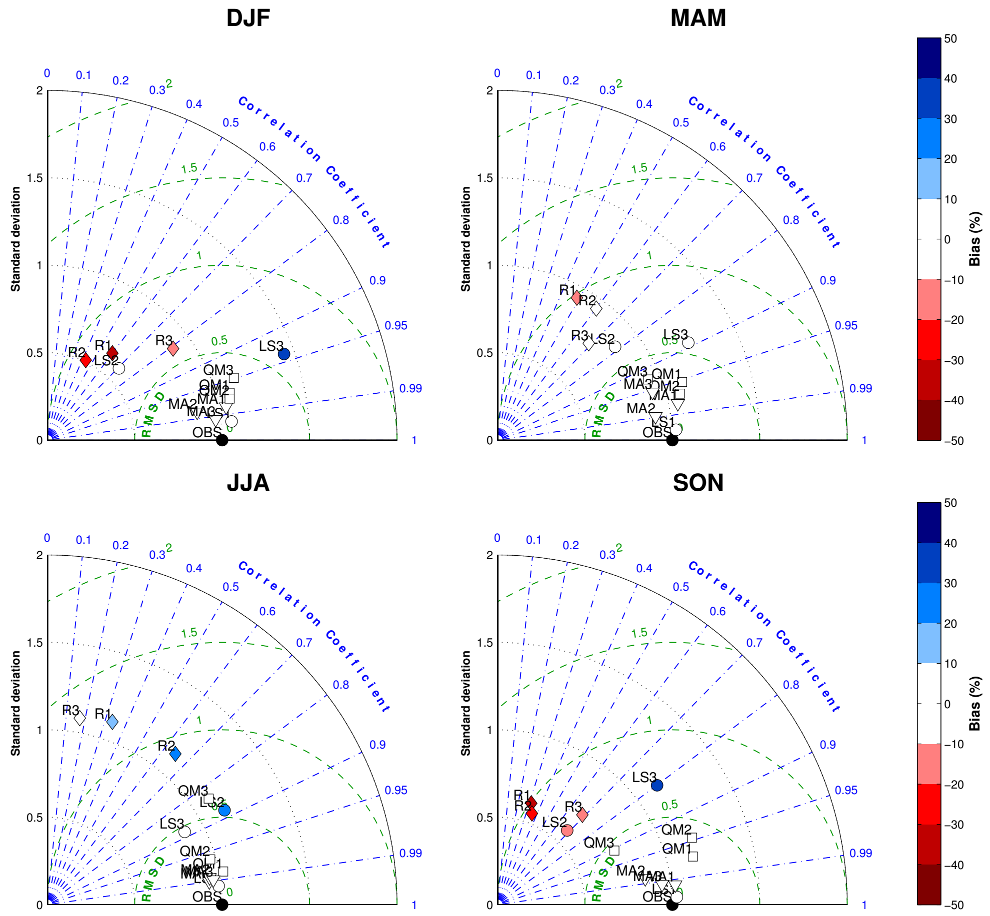

Figure 6:
Taylor diagrams for the seasonal precipitation climatology over Sardinia. Better results are closer to observation (OBS). The circles with LS are used for the linear-scaling method, the squares with QM for the quantile mapping, the triangles with MA for the MOS analogs method, while the diamonds with R for the RCM. The colours indicate the bias (in percentage respect to the Observed mean). The numbers correspond to the different indices: 1=PRCPTOT; 2=R1; 3=RX1DAY.

FUTURE SCENARIOS

In this section the future scenarios obtained from the MOS methods are presented and compared with those obtained with the COSMO-CLM model, in order to assess the consistency of climate change signal obtained with different methods.

ORVIETO

Tables 4 and 5, respectively for RCP4.5 and RCP8.5 scenarios, show the seasonal precipitation means for the period 2071-2100 along with the mean change in seasonal precipitation (DJF, MAM, JJA and SON, from left to right) between the baseline (1971-2000) and future (2071-20100) periods for the COSMO-CLM model and the three MOS methods. These results show that the climate change signal obtained using the MOS methods is generally comparable to that obtained by the COSMO-CLM model, indicating that these post-processing techniques are able to preserve the climate change signal of the RCM. A main exception regards the tendency of the MA method to give lower values than the RCM for PRCPTOT and RX1DAY indices: for RCP4.5 scenario especially in spring and in autumn, for RCP8.5 scenario also in winter. These results could be due to two main reason: (i) the seasonal bias of the RCM, that could led to an increasing of the systematic errors (as already reported in [19]), and (ii) the possible lack of robustness of the analog method in some climate change conditions since this method it is not able to produce events outside those which are present in the historical archive.

Considering the possible future changes under the RCP4.5 scenario, table 4 shows substantially a steady scenario for the $PRCPTOT$ index in all the seasons except in summer, when the RCM and the MOS methods indicate a decreased rainfall around -30%. The $R1$ index shows a decreasing signal, stronger in spring (around -20%) and summer (around -30%). Instead the $RX1DAY$ index shows positive signal in winter and spring (around 15 %), and negative in summer and autumn (respectively around -20 % and -10 %). Table 5, instead, is relative to the RCP8.5 scenario and shows a similar behaviour for total precipitation and number of rainy days, with an increase in winter, especially for $PRCPTOT$ index (around 30%), and a decrease in the other seasons, more pronounced in summer (around 70% for both the indices). Following this scenario, the maximum of daily precipitation $RX1DAY$ undergoes an increase in all the season except in summer, when a reduction of about 60% occurs.

		DJF		MAM		JJA		SON	
		Mean value	Mean change %	Mean value	Mean change %	Mean value	Mean change %	Mean value	Mean change %
PRCPTOT (mm)	**SCEN RCM**	209	3	180	-1	44	-29	191	1
	SCEN LS	192	2	186	-3	77	-36	272	0
	SCEN QM	204	7	201	3	76	-35	276	1
	SCEN MA	203	1	200	-20	72	-31	151	-19
R1 (days)	**SCEN RCM**	25	-8	23	-18	6	-28	18	-8
	SCEN LS	24	-7	23	-17	7	-32	19	-9
	SCEN QM	20	-6	18	-20	8	-38	19	-9
	SCEN MA	20	-8	21	-14	7	-30	15	-11
RX1DAY (mm/day)	**SCEN RCM**	33	17	28	16	17	-23	35	-8
	SCEN LS	29	8	29	12	30	-35	50	-9
	SCEN QM	41	12	39	16	26	-28	51	-9
	SCEN MA	35	10	33	-6	26	-10	31	-19

Table 4

Seasonal means and seasonal mean changes (%) for the three indices $PRCPTOT$, $R1$ and $RX1DAY$, for the Orvieto domain, considering the RCP4.5 scenario. The mean value for each index and for each season is averaged over the period 2071-2100, while the mean change in percentage is calculated between control (1971-2000) and future (2071-2100) periods. The values are relative to original simulation (SCEN RCM) and corrected simulations using the linear scaling (SCEN LS), quantile mapping (SCEN QM) and MOS analog (SCEN MA) approaches. For both original and corrected simulations the nearest grid point to Orvieto station has been considered.

		DJF		MAM		JJA		SON	
		Mean value	Mean change %	Mean value	Mean change %	Mean value	Mean change %	Mean value	Mean change %
PRCPTOT (mm)	**SCEN RCM**	258	28	155	-14	17	-73	178	-5
	SCEN LS	240	28	161	-16	30	-76	254	-6
	SCEN QM	264	38	179	-9	30	-75	258	-5
	SCEN MA	225	12	165	-34	36	-66	151	-20
R1 (days)	**SCEN RCM**	28	4	19	-33	3	-69	15	-23
	SCEN LS	27	4	19	-32	3	-70	16	-25
	SCEN QM	23	8	15	-33	3	-74	16	-24
	SCEN MA	22	3	16	-32	4	-64	14	-19
RX1DAY (mm/day)	**SCEN RCM**	35	25	28	18	9	-62	44	18
	SCEN LS	35	30	29	14	15	-67	64	16
	SCEN QM	49	34	41	21	14	-62	65	16
	SCEN MA	33	4	33	-5	16	-46	32	-15

Table 5

Seasonal means and seasonal mean changes (%) for the three indices $PRCPTOT$, $R1$ and $RX1DAY$, for the Orvieto domain, considering the RCP8.5 scenario. The mean value for each index and for each season is averaged over the period 2071-2100, while the mean change in percentage is calculated between control (1971-2000) and future (2071-2100) periods. The values are relative to original simulation (SCEN RCM) and corrected simulations using the linear scaling (SCEN LS), quantile mapping (SCEN QM) and MOS analog (SCEN MA) approaches. For both original and corrected simulations the nearest grid point to Orvieto station has been considered.

PO RIVER BASIN

Figure 7 shows, both for the COSMO-CLM model (first row) and for the QM method (second row), the summer $PRCPTOT$ index averaged over the baseline (1971-2000) and future (2071-2100) periods, considering the RCP4.5 scenario, and the climate change scenario given by the ratios (in percentage) of the future w.r.t. the control simulations. This in an illustrative example that indicates that, on the one hand, the future scenarios of RCM and MOS method are similar, indicating that this post-processing technique is able to preserve the climate change signal of the RCM, while, on the other hand, the absolute values are different. Indeed, the added value of the MOS scenarios lies in their absolute values.

The following figures, Fig. 8, 9 and 10, show the comparison of seasonal climate change signals between the direct model output and the QM values for, respectively, the index $PRCPTOT$, $R1$ and $RX1DAY$, considering the RCP4.5 scenario. The relative changes (i.e. the future changes relative to the historical climatology) are similar among RCM and QM, suggesting that this MOS method is able to maintain the climate change signal of the dynamical model. The climate change signal for the PRCPTOT index shows a strong decrease in summer months (around -30%) and a substantial steady (or slight increasing) signal in the other seasons. A decrease in the number of rainy days is projected in all seasons (around -10 %, more pronounced in summer, around -30/-40 %). Finally the scenarios indicate a slight increasing (between 10 and 20%) in the RX1DAY index, in all seasons except in summer where a noisy signal occurs.

For the sake of completeness, Table 6 reports the comparison between seasonal climate change signals of the RCM and all the three proposed methods, both for the RCP4.5 scenario and for the RCP8.5 scenario. These results show that the change signal obtained using LS, QM and MA methods is generally comparable to that obtained by the COSMO-CLM model for both the scenarios, indicating the capability of these post-processing techniques to preserve the climate change signal of the RCM. Only MA method shows slightly lower values, with respect to RCM, for the $RX1DAY$ index in all the seasons except winter. Moreover, in Table 6, a comparison between the RCP4.5 scenario and RCP8.5 scenario is shown. This comparison indicates that for almost all the cases (except for $PRCPTOT$ in autumn and $R1$ in winter) the sign of the climate change signal remains the same for both the scenarios, but the magnitude of the change is much greater for the RCP8.5 scenarios, as expected. In particular, the slight increment of $PRCPTOT$ (6%) projected in winter by RCP4.5, becomes a significant increase (33%) following the RCP8.5 scenario, and the decrease of all indices in summer is more pronounced, with a reduction of about 60% for $PRCPTOT$ and $R1$, and about 25% for $RX1DAY$.

		DJF Mean change %	MAM Mean change %	JJA Mean change %	SON Mean change %
PRCPTOT (mm)	SCEN RCM	6 | 33	-2 | -15	-33 | -61	6 | -5
	SCEN LS	5 | 33	-3 | -16	-35 | -63	3 | -8
	SCEN QM	9 | 43	1 | -12	-35 | -63	0 | -11
	SCEN MA	11 | 32	2 | -14	-32 | -58	5 | -3
R1 (days)	SCEN RCM	-5 | 8	-12 | -26	-36 | -61	-8 | -24
	SCEN LS	-5 | 10	-12 | -26	-36 | -62	-9 | -25
	SCEN QM	-3 | 14	-11 | -26	-37 | -63	-12 | -26
	SCEN MA	1 | 16	-5 | -18	-28 | -51	-4 | -12
RX1DAY (mm/day)	SCEN RCM	18 | 35	13 | 13	-4 | -26	15 | 21
	SCEN LS	14 | 36	12 | 11	-9 | -30	12 | 19
	SCEN QM	19 | 42	14 | 14	-5 | -25	11 | 18
	SCEN MA	19 | 20	4 | 3	-14 | -30	6 | 11

Table 6

Seasonal mean changes (%) for the three indices $PRCPTOT$, $R1$ and $RX1DAY$, over the Po river basin, both for the RCP4.5 (left of | symbol) and for the RCP8.5 (right of | symbol). The mean change in percentage is calculated between control (1971-2000) and future (2071-2100) periods. The values are relative to original simulation (SCEN RCM) and corrected simulations using the linear scaling (SCEN LS), quantile mapping (SCEN QM) and MOS analog (SCEN MA) approaches. For both original and corrected simulations the mean value, averaged over the Po basin, has been considered.

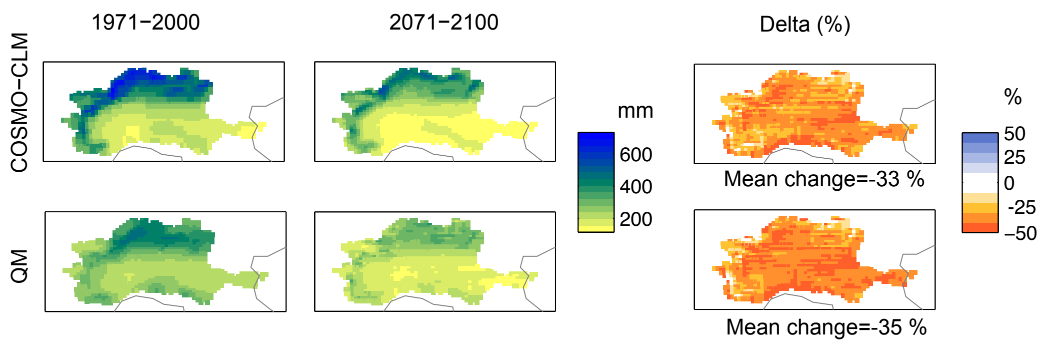

Figure 7:
Summer $PRCPTOT$ climatologies for the COSMO-CLM model (first row) and for the QM method (second row), averaged over the baseline (1971-2000) and future (2071-2100) periods and the climate change scenario given by the ratios (in percentage) of the future w.r.t. the control simulations. The considered scenario is RCP4.5.

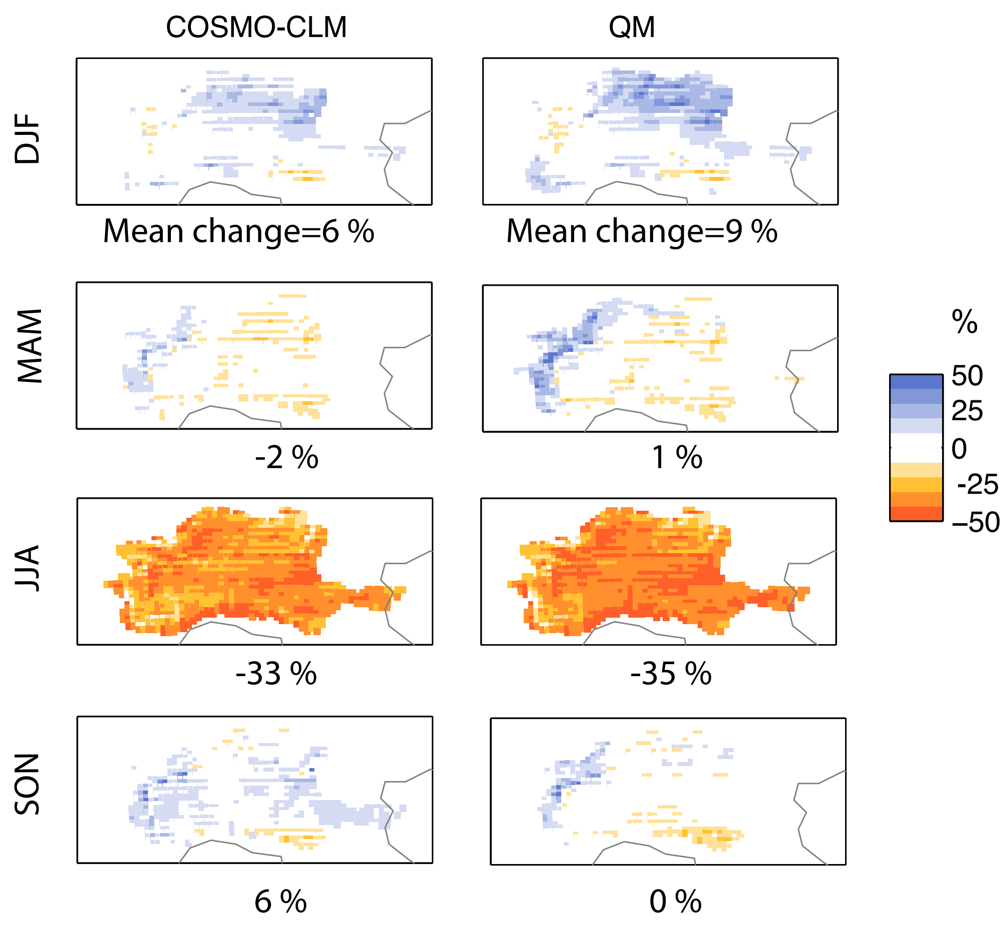

Figure 8:
Future scenarios (RCP4.5) for the $PRCPTOT$ index. Values for RCM and quantile mapping (QM) method are expressed in % of change between the baseline (1971-2000) and future (2071-2100) periods.

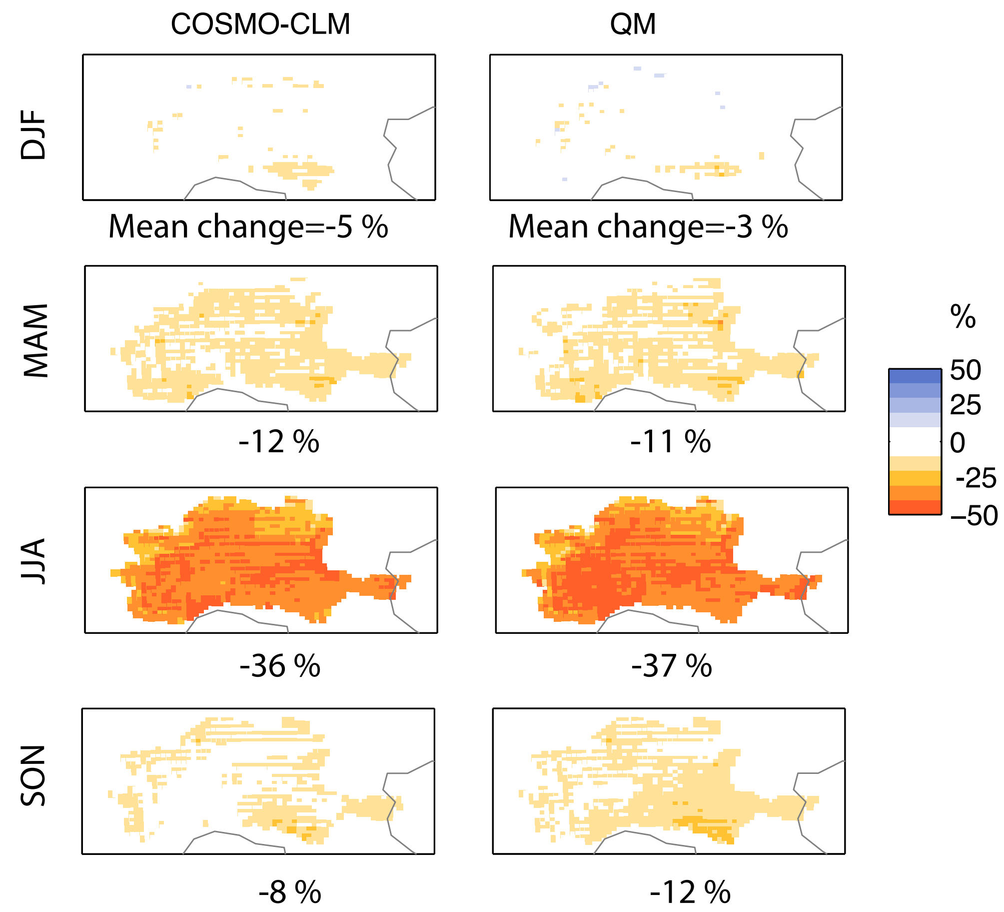

Figure 9:
The same as Fig. 8 for the $R1$ index.

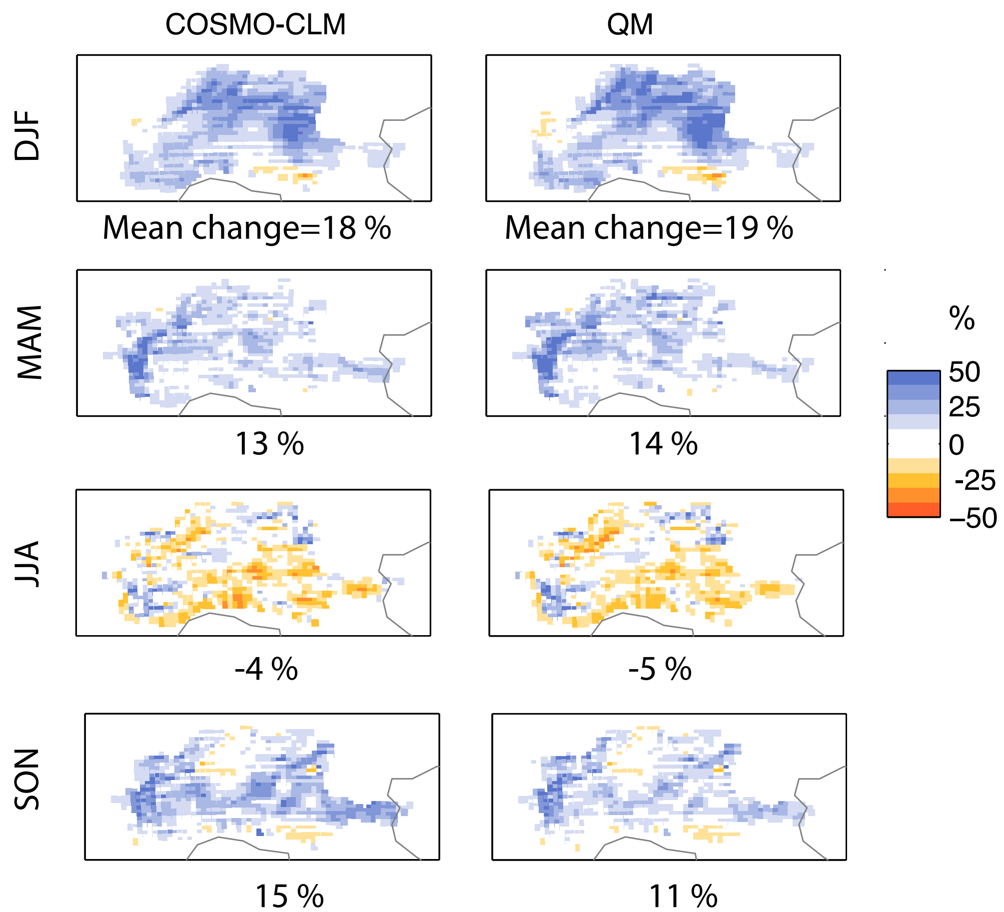

Figure 10:
The same as Fig. 8 for the $RX1DAY$ index.

SARDINIA

In the figures 11, 12 and 13 the comparison of seasonal climate change signals between the direct model output and the QM values is shown respectively for the index $PRCPTOT$, $R1$ and $RX1DAY$, considering the RCP8.5 scenario. Also for the Sardinia island the relative changes (i.e. the future changes relative to the historical climatology), generally are similar among RCM and QM, suggesting that this MOS method preserves the climate change signal of the dynamical model. The climate change signal projected by RCP8.5 scenario for the PRCPTOT index (Fig. 11) shows a significant increase in winter, around 60% (with slightly higher values for the QM method), and a decrease in the other seasons, stronger in summer (around -80%). A similar pattern appears for the R1 index (Fig. 12), except in winter, when a lower increase than the $PRCPTOT$ occurs (about 20%). The RX1DAY shows a noisier spatial pattern of climate change signal especially in spring, with a negative average value, and autumn, with a positive average value. In winter a general increase is projected, and there is a strong positive signal in the west part of the domain, while there is a substantially steady signal in the east part. A strong decrease is shown for the summer scenario (more than 60%). Table 7 summarizes seasonal mean changes (%) for the three indices $PRCPTOT$, $R1$ and $RX1DAY$, for all the proposed methods and for both the scenarios (RCP4.5 and RCP8.5). The comparison between the two scenarios shows that for almost all the cases (except for $PRCPTOT$ in autumn and $RX1DAY$ in spring) the sign of the climate change signal remains the same, but the magnitude of the change is much greater for the RCP8.5 scenario. Analyzing table 7, emerges that both LS and QM methods are able to preserve the climate change signal projected by RCM, while the MA technique shows a quite different change signal with respect to RCM, especially in winter for all the indices and in autumn for the $PRCPTOT$ index.

		DJF Mean change %	MAM Mean change %	JJA Mean change %	SON Mean change %
PRCPTOT (mm)	SCEN RCM	41 | 56	-8 | - 27	-68 | -81	23 | -14
	SCEN LS	38 | 81	-22 | -23	-77 | -83	30 | -3
	SCEN QM	37 | 66	-22 | - 22	-78 | -83	23 | -10
	SCEN MA	-3 | -6	-4 | -22	-30 | -65	-34 | -47
R1 (days)	SCEN RCM	20 | 19	-11 | -30	-67 | -83	-4 | -35
	SCEN LS	20 | 19	-20 | -29	-74 | -83	-2 | -34
	SCEN QM	30 | 27	-19 | -26	-75 | -84	-2 | -32
	SCEN MA	-4 | -10	-9 | -27	-28 | -65	-27 | -41
RX1DAY (mm/day)	SCEN RCM	20 | 30	6 | -7	-48 | -63	24 | 14
	SCEN LS	21 | 52	-3 | -1	-61 | -67	34 | 28
	SCEN QM	3 | 25	-9 | -5	-64 | -68	26 | 21
	SCEN MA	1 | -1	7 | -3	-18 | -47	-21 | -25

Table 7

Seasonal mean changes (%) for the three indices $PRCPTOT$, $R1$ and $RX1DAY$, over Sardinia, both for the RCP4.5 (left of | symbol) and for the RCP8.5 (right of | symbol). The mean change in percentage is calculated between control (1971-2000) and future (2071-2100) periods. The values are relative to original simulation (SCEN RCM) and corrected simulations using the linear scaling (SCEN LS), quantile mapping (SCEN QM) and MOS analog (SCEN MA) approaches. For both original and corrected simulations the mean value, averaged over the Po basin, has been considered.

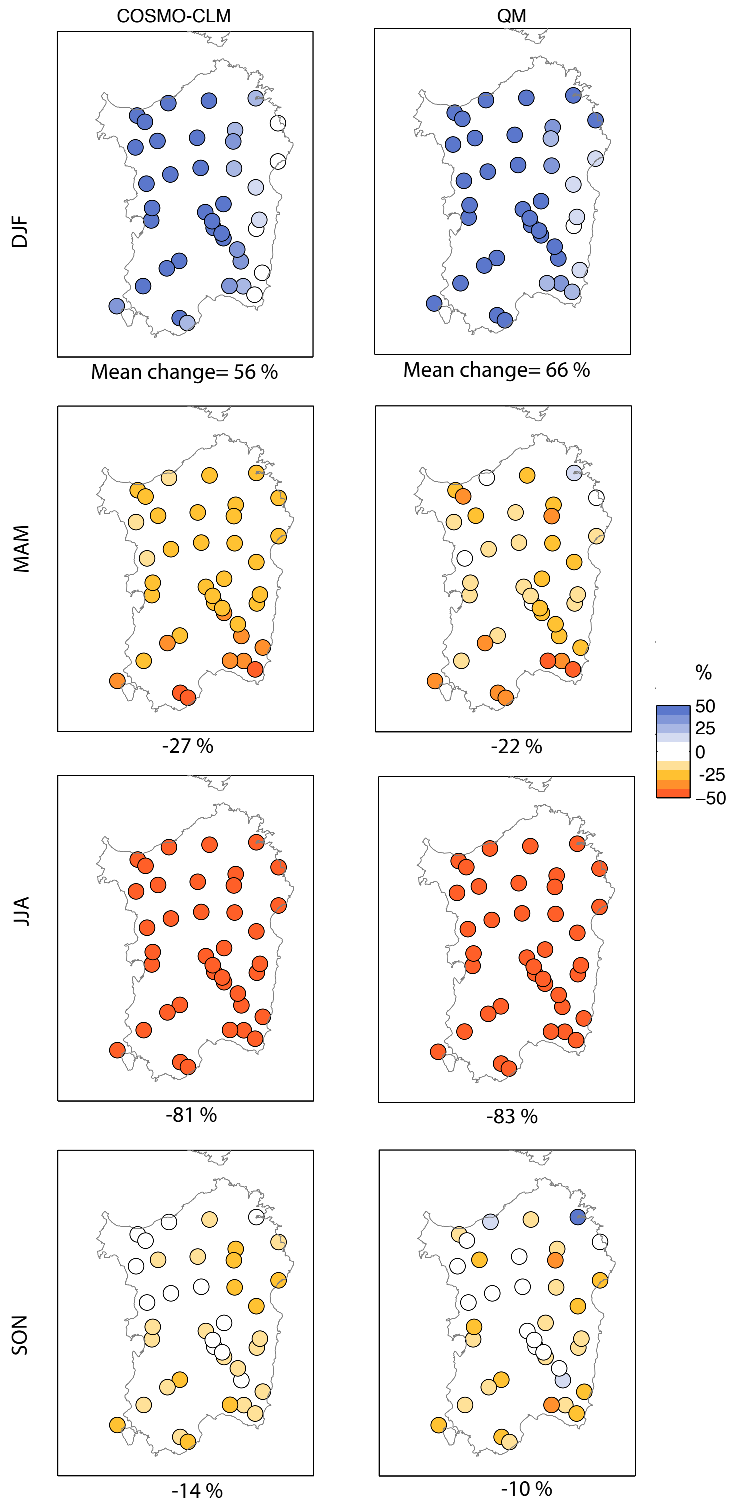

Figure 11:
Future scenarios (RCP8.5) for the $PRCPTOT$ index. Values for RCM and quantile mapping (QM) method are expressed in % of change between the baseline (1971-2000) and future (2071-2100) periods.

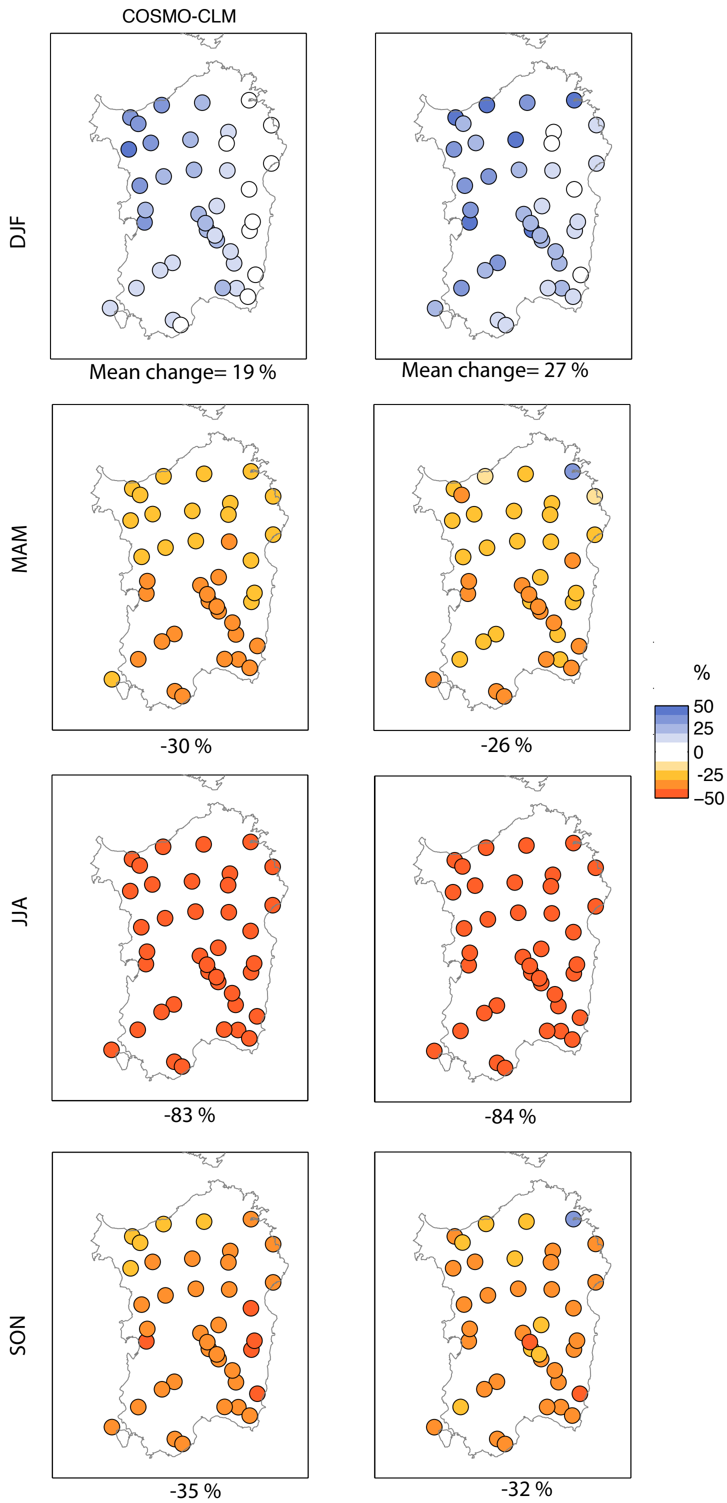

Figure 12:
The same as Fig. 8 for the $R1$ index.

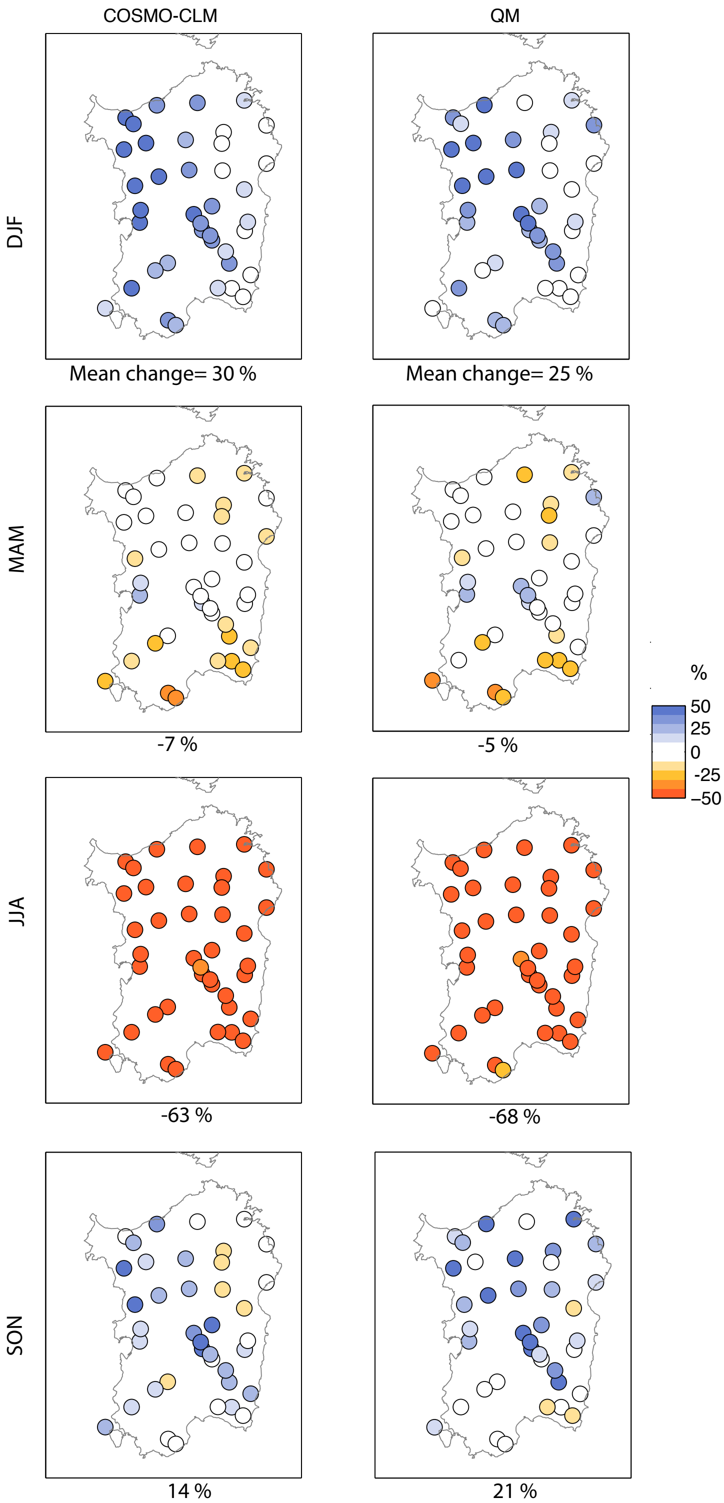

Figure 13:
The same as Fig. 8 for the $RX1DAY$ index.

CONCLUSION

In this report we have investigated (i) the applicability of three MOS techniques (LS, QM and MA) to the CMCC-CM driven COSMO-CLM model (ii) the possible future changes and the consistency among direct model and post-processed scenarios. This study extend the analysis of Turco et al. (2013a, [19]), in which the focus was on the analysis of these MOS methods applied to the ERA40-driven COSMO-CLM.

Here, we show that the validation against the observed data in three different domains (Orvieto, Po river basin and Sardinia island) confirms that the MOS downscaled values clearly outperform the uncalibrated RCM outputs, with better performance of the QM method in most of the cases.

Generally, the climate change signal is similar among the dynamical model outputs ad the statistical model ones. Note that the relative changes (i.e. the future changes relative to the historical climatology) should be similar among RCM and MOS. Instead, the added values of the MOS scenarios lie in their absolute values (contrary to the relative changes). This again suggests that the MOS outputs may be very useful for those users who require high-resolution data where systematic errors are reduced.

The projected changes are quite consistent over the three domains: they generally indicate a strong decrease in summer, regardless of the scenario (RCP4.5 or RCP8.5), domain, downscaling method or precipitation indices. Instead a noisier climate change signal for the other seasons/regions/scenarios. We underline that, in spite of the rather agreement of the simulated fields in the control period, the overall uncertainties in future rainfall climate scenarios remain quite large, suggesting that these future scenarios should be taken with caution.

Bibliography

[1] R.E. Benestad, I. Hanssen-Bauer, and D. Chen. *Empirical-Statistical Downscaling*. World Scientific Publishers, 2008.

[2] D.R. Easterling, G.A. Meehl, C. Parmesan, S.A. Changnon, T.R. Karl, and L.O. Mearns. Climate extremes: Observations, modeling, and impacts. *Science*, 289(5487):2068–2074, 2000.

[3] C. Frei and C. Schär. A precipitation climatology of the alps from high-resolution raingauge observations. *International Journal of Climatology*, 18(8):873–900, 1998.

[4] F. Giorgi and L.O. Mearns. Approaches to the Simulation of Regional Climate Change - A review. *Reviews of Geophysics*, 29(2):191–216, 1991.

[5] O. Gutjahr and G. Heinemann. Comparing precipitation bias correction methods for high-resolution regional climate simulations using cosmo-clm. *Theoretical and Applied Climatology*, pages 1–19, 2013.

[6] M.R. Haylock, N. Hofstra, A.M.G. Klein Tank, E.J. Klok, P.D. Jones, and M. New. A European daily high-resolution gridded data set of surface temperature and precipitation for 1950-2006. *J. Geophys. Res.*, 113(D20):D20119, October 2008.

[7] A.V.M. Ines and J.W. Hansen. Bias correction of daily gcm rainfall for crop simulation studies. *Agricultural and Forest Meteorology*, 138:44–53, 2006.

[8] D. Maraun, F. Wetterhall, A.M. Ireson, R.E. Chandler, E.J. Kendon, M. Widmann, S. Brienen, H.W. Rust, T. Sauter, M. Themessl, V.K.C. Venema, K.P. Chun, C.M. Goodess, R.G. Jones, C. Onof, M. Vrac, and I. Thiele-Eich. Precipitation Downscaling under Climate Change: Recent Developments to Bridge the Gap Between Dynamical Downscaling Models and the End User. *Reviews of Geophysics*, 48, 2010.

[9] B. Orlowsky and S.I. Seneviratne. Global changes in extreme events: regional and seasonal dimension. *Climatic Change*, 110(3-4):669–696, July 2011.

[10] C. Piani, J.O. Haerter, and E. Coppola. Statistical bias correction for daily precipitation in regional climate models over europe. *Theoretical and Applied Climatology*, 99(1-2):187–192, 2009.

[11] C. Piani, G.P. Weedon, M. Best, S.M. Gomes, P. Viterbo, S. Hagemann, and J.O. Haerter. Statistical bias correction of global simulated daily precipitation and temperature for the application of hydrological models. *Journal of Hydrology*, 395, 2010.

[12] B. Rockel, A. Will, and A. Hense. The regional climate model cosmo-clm (cclm). *Meteorologische Zeitschrift*, 17(4):347–348, 2008.

[13] M. Rummukainen. Changes in climate and weather extremes in the 21st century. *Wiley Interdisciplinary Reviews: Climate Change*, 3(2):115–129, 2012.

[14] E. Scoccimarro, S. Gualdi, A. Bellucci, A. Sanna, P.G. Fogli, E. Manzini, M. Vichi, P. Oddo, and A. Navarra. Effects of tropical cyclones on ocean heat transport in a high resolution coupled general circulation model. *Journal of Climate*, 24:4368–4384, 2011.

[15] J. Steppeler, G. Doms, U. Schättler, H. W. Bitzer, A. Gassmann, U. Damrath, and G. Gregoric. Meso-gamma scale forecasts using the nonhydrostatic model lm. *Meteorology and Atmospheric Physics*, 82:75–96, 2003.

[16] K.E. Taylor. Summarizing multiple aspects of model performance in a single diagram. *J. Geophys. Res.*, 106(D7):7183–7192, 2001.

[17] C. Teutschbein and J. Seibert. Bias correction of regional climate model simulations for hydrological climate-change impact studies: Review and evaluation of different methods. *Journal of Hydrology*, 2012.

[18] M. Turco, P. Quintana-Seguí, M.C. Llasat, S. Herrera, and J.M. Gutiérrez. Testing MOS precipitation downscaling for ENSEMBLES regional climate models over Spain. *Journal of Geophysical Research*, 116(D18):1–14, 2011.

[19] M. Turco, A. L. Zollo, G. Rianna, Cattaneo L., R. Vezzoli, and P. Mercogliano. Post-processing methods for COSMO-CLM precipitation over Italy. Technical report, CMCC, 2013.

[20] M. Turco, A. L. Zollo, C. Ronchi, C. De Luigi, and P. Mercogliano. Assessing gridded observations for daily precipitation extremes in the Alps with a focus on northwest Italy. *Natural Hazards and Earth System Science*, 13(6):1457–1468, 2013.

[21] R. Wilby, S. Charles, E. Zorita, and B. Timbal. Guidelines for use of climate scenarios developed from statistical downscaling methods. Technical report, IPCC, 2004.

[22] A.L. Zollo, M. Montesarchio, M.P. Manzi, L. Cattaneo, E. Bucchignani, and P. Mercogliano. Assessment of COSMO-CLM Performances in Simulating the Past Climate of Italy. Technical report, CMCC, 2012.